Cement and Concrete Research 40 (2010) 347–351

Contents lists available at ScienceDirect

Cement and Concrete Research

journal homepage: http://ees.elsevier.com/CEMCON/default.asp

Impact resistance of poly(vinyl alcohol) fiber reinforced high-performance organic aggregate cementitious material

Bo Xu [a,*], Houssam A. Toutanji [a], John Gilbert [b]

[a] Department of Civil and Environmental Engineering, University of Alabama in Huntsville, Huntsville, AL, USA
[b] Department of Mechanical and Aerospace Engineering University of Alabama in Huntsville, Huntsville, AL, USA

ARTICLE INFO

Article history:
Received 6 March 2009
Accepted 9 September 2009

Keywords:
PVB
PVA fiber
Impact energy
Concrete
Hydrogen bond

ABSTRACT

Poly(vinyl butyral) (PVB) which has many special engineering aggregate properties such as super lightweight, physical toughness, adhesion to a variety of surfaces and energy-absorbing characteristics is utilized as the sole aggregate in this study to develop a novel cementitious composite reinforced with Poly (vinyl alcohol) (PVA) fiber. Impact energy absorption capacity is evaluated based on the Charpy impact test. The results show that PVB composite material has lower density but higher impact energy absorption capability compared with conventional lightweight concrete and regular concrete. The addition of PVA fiber improves the impact resistance with fiber volume fractions. The remarkable change in the interfacial bond strength contributed by the non-covalent bond such as hydrogen bond and ether interactions at the interfaces between fiber, aggregate and matrix contributes to the improvement of the impact resistant capacity. A model based on fiber bridging mechanics and the rule of mixtures is developed to characterize the impact energy. A good correlation was obtained for the materials tested when experimental results are compared to those predicted by the developed model.

1. Introduction

Fiber reinforced concrete (FRC) consists of three phases: matrix (cement paste), fiber and aggregate. Many studies have shown that fiber reinforced concrete (FRC) has higher energy absorption capacity compared with plain concrete. Impact resistance can be increased substantially with the addition of randomly distributed fibers to concrete [1]. Wang, N. and his colleagues [2] tested on the impact resistance of small concrete beams reinforced with different volumes of both polypropylene and steel fibers. Mindess, S. et al. [3] evaluated the impact resistance of precast concrete box units reinforced with polyolefin fibers. Statistical variation of impact resistance of steel fiber reinforced concrete subjected to drop weight type test was reported by Natraja, M.C. et al. [4]. Arisoy, B. [5] studied the impact resistance of lightweight concrete reinforced with PVA fiber.

However, the impact resistance capacity of conventional concrete reinforced with steel or polymer fiber is limited due to poor bonding between the fiber and matrix. Fiber/matrix debonding by tensile or shear type of deformation and fiber sliding wear are the dominant failure mechanisms [6]. In addition to that, weak bonding between the aggregate/matrix at the interfacial transition zone (ITZ) limited the performance of impact resistance capacity of the concrete.

Fiber reinforced concrete (FRC) can be considered at four structural levels [7]. The chemical structure of both phases and van der Waals forces, acid-base interactions, covalent bonds or electrostatic intermolecular attraction are considered to be molecular level. It determines the bond strength, interfacial shear stress, critical energy release rate on micro level and also affects the mechanical properties of the composite material on meso and structural level which take into account the fiber distribution and bulk material performance.

Conventional methods have been introduced to improve the aggregate/matrix bonding in the ITZ [8–13], but the effects of those methods are limited because they do not significantly increase the interactions between the atoms and molecules. Steel and glass fiber have good mechanical properties such as tensile strength and elastic modulus, however, they have a limitation on the interfacial bond between fiber and matrix.

Prior research [14,15] has shown that by employing poly(vinyl butyral) (PVB) as a total replacement for aggregate and using PVA fiber as reinforcement, cementitious composite materials display strong interactions at the molecular level, resulting in improved ductility and fracture toughness with increasing fiber volume fraction.

Both PVB and PVA contain hydroxyl groups which have the potential to form hydrogen bond between molecules, or within different parts of a single molecule. The molecular structure of PVB and PVA are shown in Figs. 1 and 2. This special feature provides remarkable changes in the surface bond strength, not only between the aggregate and the matrix, but also between the fiber reinforcement and the matrix and aggregates. The adhesion feature is illustrated in Fig. 3. Additionally, the ether oxygen functional group acts as a weak base and can interact with Lewis acids and electropositive materials such as C–S–H or magnesium.

* Corresponding author. Tel.: +1 212 839 7416.
E-mail address: bx0001@uah.edu (B. Xu).

0008-8846/$ – see front matter © 2009 Elsevier Ltd. All rights reserved.
doi:10.1016/j.cemconres.2009.09.006

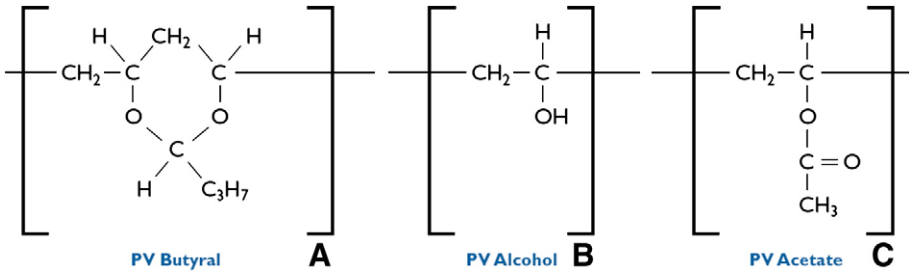

Fig. 1. Structure of poly(vinyl butyral) (PVB) [16].

The purpose of this research was to test the impact resistance of PVB concrete reinforced with PVA fiber and compare it with lightweight concrete and normal weight concrete. A model was developed to estimate the impact energy absorbed by the fiber reinforced composite in the Charpy impact test.

2. Theoretical aspects

2.1. Critical fiber length

Consider a model composite consisting of a fiber of length l embedded in a matrix. If this fiber is pulled out, the adhesion between matrix and fiber will produce a shear stress parallel to the fiber surface. The total force acting on the fiber as a result of this stress is given by $2\pi r_f l\tau_i$, where r_f is the fiber radius and τ_i is the maximum shear stress that the interface can support. Let σ_{fu} be the fiber tensile fracture stress. So the maximum force caused by this normal stress on the fiber is $\pi r_f^2\sigma_{fu}$. When the normal force is greater than the shear force, the fiber will break. Otherwise, the fiber will pull out from the matrix. Fiber pullout can be expressed as follows (Eqs. (1) and (2)) [18]:

$$\pi r_f^2\sigma_{fu} > 2\pi r_f\frac{l}{2}\tau_i \tag{1}$$

or

$$\frac{\sigma_{fu}}{2\tau_i} > \frac{l}{2r_f} = \frac{l}{d} \tag{2}$$

where d is the fiber diameter and the ratio l/d is the fiber aspect ratio.

Therefore the critical fiber length for a given fiber diameter can be expressed by Eq. (3) as the following:

$$\frac{l_c}{d} = \frac{\sigma_{fu}}{2\tau_i} \tag{3}$$

2.2. Fiber pullout energy

Chawla, K.K. [18] estimated the work done in pulling out an isolated fiber in the following way. He assumes that the fiber with a diameter d is pulled out through a distance x against an interfacial frictional shear stress, τ_i. Then the total force at that instant on the debonded fiber surface opposing the pullout is $\tau_i\pi d(k-x)$, where k is the fiber embedded length. When the fiber is further pulled out a distance dx, the work done by this force is $\tau_i\pi d(k-x)dx$. The total work U_f done in pulling out the fiber over the distance k can be obtained by integration as Eq. (4). Therefore,

$$U_f = \int_0^k \tau_i\pi d(k-x)dx = \frac{\tau_i\pi dk^2}{2} \tag{4}$$

The pullout length of the fiber can vary between a minimum of 0 and a maximum of $l_c/2$. where l_c is the critical fiber length which can be calculated by Eq. (3).

Integrating dk gives the average work of pullout per fiber as Eq. (5):

$$W_{fp} = \frac{1}{l_c/2}\int_0^{l_c/2}\frac{\tau_i\pi dk^2}{2}dk = \frac{\tau_i\pi dl_c^2}{24} \tag{5}$$

3. Sample preparation and testing methods

3.1. Mix proportions

The water to cementitious material ratio of all groups were kept at a constant of 0.4. The fiber volume fractions V_f were varied from 0 to 0.9% in each group. For the normal weight concrete, the cement to sand ratio was 1:3. For the lightweight concrete, the density was about 1500 kg/m^3 (93.6 PCF), which was almost the same as the PVB composite mix. The mix proportion is listed in Table 1.

The cement used was ASTM Type I normal Portland cement. The metakaolin (MK) conformed with the ASTM C-618 [19], Class N Specifications for Natural and Calcined Pozzolans. Sika ViscoCrete 2100 superplasticizer, which meets the requirements for ASTM C-494 Types A and F [20] was used. The Poly(vinyl butyral) (PVB) was Mowital B75H and Butvar B-79. Mowital was produced by Kuraray Specialities Europe (KSE). Butvar B-79 was provided by Solutia Inc. Table 2 lists some properties of PVB products.

The poly(vinyl alcohol) (PVA) fibers used, type RECS15, were manufactured by Kuraray Co. Ltd of Japan and have the properties listed in Table 3.

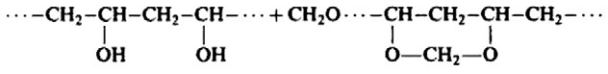

Fig. 2. Formal groups of PVA fiber [17].

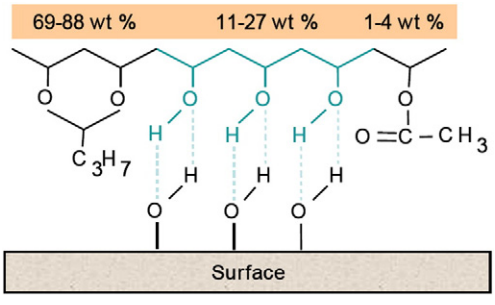

Fig. 3. Adhesion to substrates by hydrogen bond [14,15].

Table 1
Proportion of the mix (kg/m^3).

	Mix number	Cement	MK	Beach sand	Lightweight sand	B-79	M-B75H	Water	SIKA	PVA fiber	w/c	V_f (%)
Normal weight concrete	C1	558		1674				223			0.4	0
	C2	558		1674				223		4.1	0.4	0.3
	C3	558		1674				223		8.2	0.4	0.6
	C4	558		1674				223		12.3	0.4	0.9
Lightweight concrete	L1	437		147	728			175			0.4	0
	L2	437		147	728			175		3.9	0.4	0.3
	L3	437		147	728			175		7.8	0.4	0.6
	L4	437		147	728			175		11.7	0.4	0.9
PVB composite	M1	833.3	79.4			182.5	119.0	363.5	11.9		0.4	0
	M2	833.3	79.4			182.5	119.0	363.5	11.9	4.2	0.4	0.3
	M3	833.3	79.4			182.5	119.0	363.5	11.9	8.3	0.4	0.6
	M4	833.3	79.4			182.5	119.0	363.5	11.9	12.5	0.4	0.9

3.2. Testing methods

The Charpy U-notch test refers to the ASTM E23 [21], Standard Test Methods for Notched Bar Impact Testing of Metallic Material and was used to determine fracture energy. The configurations of the specimen for the Charpy impact test are shown in Fig. 4. The loading configuration is shown is Fig. 5. Tinius Olsen "Change-O-Matic" impact testing machine (Fig. 6) was used in this test. After setting the specimen, the pendulum was released from a height y_1 and swinged through the specimen to a height y_2. Assuming negligible friction and aerodynamic drag, the energy absorbed by the specimen was equal to the height difference times the weight of the pendulum.

3.3. Experiment results

The results in Table 4 and Fig. 7 show that PVB composite with a lower density has an average impact energy of 14.92 J (11.00 ft-lb), which is higher than for lightweight concrete of 9.83 J (7.25 ft-lb) and normal weight concrete of 11.53 J (8.50 ft-lb). The impact energy increased with the addition of the PVA fiber to 0.9% by volume. The impact energy started to decrease after the fiber volume fraction continuously increased to 1.2%. This was due to the bad workability and non-compacted status of the material at pouring which involved a lot of air bubbles and voids. However, PVB concrete showed a higher improvement of impact energy at the lower level of fiber volume fraction (~0.9%), which shows that the PVB composite matrix had a better bond with PVA fiber. Note that when the fiber volume fraction was increased to 0.9%, the impact energy had a tremendous increase. This was due to multi-crack planes forming instead of the single crack at the cross section, where more surface energy was dissipated.

Table 2
Special properties of PVB products [16].

Property	Units	Condition	Value
PVOH[a] content	%	B-79	11.5–13.5
		M-B75H	11–27
Specific gravity	–	B-79	1.083
		M-B75H	1.1
Tensile yield strength	MPa	B-79	40–47
		M-B75H	
Elastic modulus	MPa × 103	B-79	1.93–2.0
		M-B75H	
Impact strength	J m-1	Izod, notched, 1.25 × 1.25 cm,	42.7
		B-79	–
		M-B75H	
Glass transition temperature	°C	B-79	62–72
		M-B75H	73

[a] PVOH is the poly(vinyl alcohol) (PVA) residual in the PVB polymer.

Table 3
Physical and mechanical property of PVA fiber.

Fiber type	Diameter (mm)	Thickness (dtex)	Cut length (mm)	Tensile strength (N/mm^2)	Elongation (%)	Young's Modulus (kN/mm^2)	Specific Gravity
RECS15	0.04	15	8	1600	7	40	1.3

4. Modeling the impact energy absorption

The energy absorption in a notched beam subjected to impact is dominated by the independent contribution of three major factors: energy absorption due to the matrix crack, energy absorption due to the fiber/matrix debonding and energy absorption due to the fiber sliding.

Specifically, at the beginning of the loading process the matrix and fiber work together to resist the impact load. In this case, the stress is transferred from the matrix to the fiber via the fiber/matrix interface. But when loads are increased to the point at which the matrix begins to crack, the stress is transferred to the fibers alone. Fiber/matrix debonding and sliding occurs when the mismatch of the axial strain between fiber and matrix reaches a critical value [22]. With the

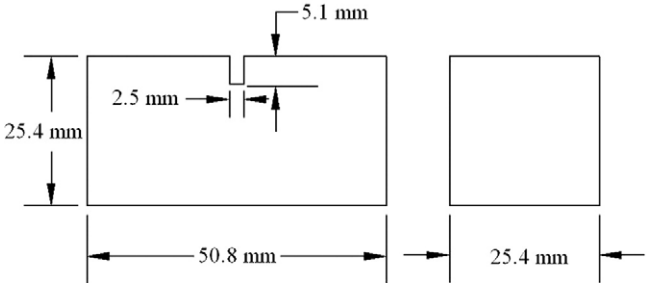

Fig. 4. Charpy U-notch specimen.

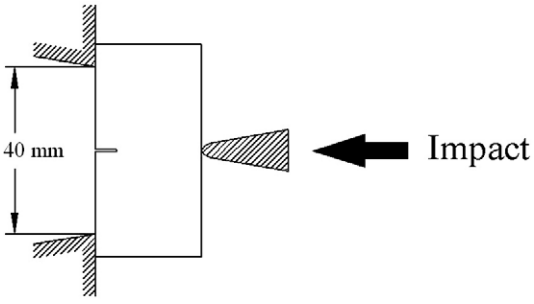

Fig. 5. Loading configuration for Charpy U-notch test.

Fig. 6. Tinius Olsen "Change-O-Matic" impact testing machine.

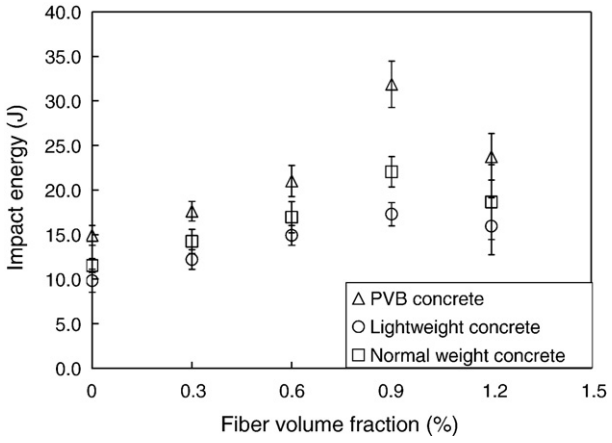

Fig. 7. The impact energy with the fiber volume fraction.

continuing increase in the deformation, fibers slide out of the matrix and failure occurs.

Although usually the fiber pullout process consists of three processes, fiber/matrix working together, fiber/matrix debonding and fiber/matrix sliding, but in this model, the latter two processes are combined as one. Fiber/matrix debonding is considered as the early stage in the fiber sliding. Fiber/matrix interfacial shear strength is deemed as an equivalent shear bond strength, although it varies along the fiber length [23,24]. According to the rule of mixtures [25], total energy absorbed by the system is expressed in Eq. (6)

$$U = U_m V_m + U_f V_f \tag{6}$$

or it can be expressed as Eq. (7)

$$U = U_m V_m + \sum_{i=1}^{N_f} U_{fi} \tag{7}$$

or Eq. (8)

$$U = U_m V_m + N_f U_{fi} \tag{8}$$

Where U_m is the crack energy absorbed by the matrix with no fiber. V_m is the volume fraction of the matrix. N_f is the number of fibers in the crack plane. U_{fi} in Eq. (9) is energy per fiber which can be calculated by Eq. (5)

$$U_{fi} = W_{fp} = \frac{1}{l_c/2}\int_0^{l_c/2} \frac{\tau_i \pi d k^2}{2} dk = \frac{\tau_i \pi d l_c^2}{24} \tag{9}$$

Therefore, total energy can be expressed as Eq. (10)

$$U = U_m V_m + N_f \frac{\tau_i \pi d l_c^2}{24} \tag{10}$$

because in Eq. (11),

$$N_f \frac{\pi d^2}{4} = A V_f \tag{11}$$

Table 4
Impact resistance.

	Density (kg/m^3)	Impact energy (J)				
		V_f=0%	V_f=0.3%	V_f=0.6%	V_f=0.9%	V_f=1.2%
PVB composite	1548.23	14.92	17.63	21.02	31.87	23.71
Lightweight concrete	1491.02	9.83	12.20	14.92	17.29	15.93
Normal weight concrete	2456.31	11.53	14.24	16.95	22.04	18.65

Therefore, the number of fibers in the crack plane can be expressed as Eq. (12)

$$N_f = \frac{4AV_f}{\pi d^2} \tag{12}$$

where A is the area of the crack plane calculated as the cross-section area.

Hence, substituting Eq. (12) into Eq. (10) gives,

$$U = U_m V_m + \frac{\tau_i l_c^2 A V_f}{6d} \tag{13}$$

In order to calculate the impact energy from (Eq. (13)), it is necessary to obtain the interfacial bond strength, τ_i, which is defined as the friction between the fiber and the matrix.

Although, the ultimate tensile strength was not measured directly herein, it can be estimated by the modulus of rupture R (Eq. (15)). Moreover, it is assumed that the tensile strength and the modulus of rupture of fiber reinforced concrete are very similar to those of plain concrete, since the volume fractions are relatively low (<2%) [5].

The tensile stress at the extreme fiber in the mid span can be expressed as the summation of the tensile stress of the matrix and the fiber. Hence, the interfacial bond strength can be obtained from Eqs. (14) and (15), provided that a flexural test is performed to obtain the flexural stress

$$\sigma = \frac{1}{2} V_f g \tau \left(\frac{L_f}{d_f}\right) + \sigma_m (1 - V_f) \tag{14}$$

$$\sigma = R = \frac{M \cdot c}{I} \tag{15}$$

Table 5 shows the shear bond strength for the three materials tested, with and without fiber. It is evident that the PVB group has a higher interfacial bond strength than that of lightweight and normal concrete. Table 6 lists the theoretical results obtained from these

Table 5
Interfacial bond strength.

	Flexural stress σ (MPa)				g[a]	L_f/d_f	τ (MPa)
	V_f=0%	V_f=0.3%	V_f=0.6%	V_f=0.9%			
PVB composite	4.07	5.36	6.63	7.56	1.5	200	2.79
Lightweight concrete	2.35	3.02	3.70	4.03	1.5	200	1.42
Normal weight concrete	2.06	3.02	3.58	4.44	1.5	200	1.86

[a] According to Li [26].

Table 6
Comparison of impact energy.

	Source	Impact energy (J)			
		$V_f = 0\%$	$V_f = 0.3\%$	$V_f = 0.6\%$	$V_f = 0.9\%$
PVB concrete	Calculation	14.92	17.17	19.41	21.66
	Test	14.92	17.63	21.02	31.87
Lightweight concrete	Calculation	9.83	14.31	18.79	23.26
	Test	9.83	12.20	14.92	17.29
Normal weight concrete	Calculation	11.53	14.93	18.34	21.74
	Test	11.53	14.24	16.95	22.04

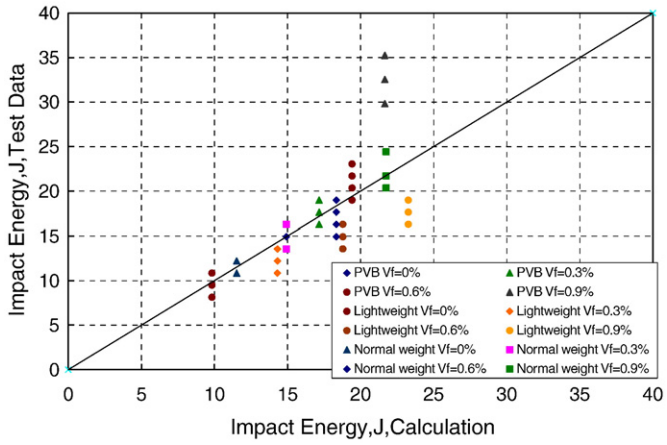

Fig. 8. Comparison of impact energy.

expressions along with the average values obtained from the tests. Fig. 8 includes data taken from all specimens (3) of each type, clearly illustrating that the results from the model compare well with the test data.

At the lower fiber volume fraction rate (below 0.6%), the testing data have a good agreement with the calculation. At this stage, fiber and matrix systems followed the linear law stated in the model. After that, the model tended to give a lower evaluation of impact energy for PVB composite when the fiber volume fraction was increased to 0.9%. This was due to the increase in the fiber amount and interfacial bond strength which caused the formation of multi-crack planes instead of a single crack plane, where more energy was dissipated. Further increase in the fiber caused a non-compact status of the material, which reduced the impact energy absorption capacity and involved other issues that were not considered in the model.

5. Conclusions

In this study, poly(vinyl butyral) (PVB) and PVA fibers were used as fine aggregate and reinforcement to develop a novel cementitious material. The Charpy impact test was performed to show the energy absorption capacity of this new material and the effect of the reinforcement from PVA fiber. Light weight concrete with the same density and normal weight concrete were developed to make a comparison. An impact model was developed. Several conclusions can be drawn from this study:

1. PVB composite has a higher energy absorption capacity compared with conventional lightweight concrete and normal weight concrete. This implies that PVB, when used as an aggregate, has a higher interfacial bond energy with cement matrix. This is attributed to the fact that PVB contains hydroxyl groups which have potential to form hydrogen bonds between molecules. Additional effects on the cement matrix itself may occur through available ether group interactions which may alter the cement matrix structure or nucleation reaction.
2. By adding PVA fiber to the matrix at a lower volume fraction, cementitious material had an increased capability in resisting the impact load and absorbing impact energy. Compared with conventional lightweight concrete and normal weight concrete, PVB composite has better energy absorption capacity with the addition of PVA fiber.
3. The higher improvement in the impact energy and the generation of multi-cracks in PVB composite shows that PVB composite had a higher interfacial bond strength with PVA fiber compared with the lightweight concrete and the normal weight concrete.
4. The energy model developed in this study shows good correlation with the testing data at the lower fiber volume fraction(~0.6%). The deviation at the higher volume fraction was caused by the formation of multi-crack planes where more energy is dissipated.

References

[1] Y. Mohammadi, R. Carkon-Azad, S.P. Singh, S.K. Kaushik, Impact resistance of steel fibrous concrete containing fibres of mixed aspect ratio, Construction and Building Materials 23 (1) (2009) 183–189.
[2] N. Wang, S. Mindess, K. Ko, Fiber reinforced concrete beams under impact loading, Cement and Concrete Research 26 (3) (1996) 363–376.
[3] S. Mindessa, N. Wanga, L.D. Richb, D.R. Morganc, Impact resistance of polyolefin fiber reinforced precast units, Cement and Concrete Composites 20 (5) (1998) 387–392.
[4] M.C. Natraja, N. Dhang, A.P. Gupta, Statistical variations in impact resistance of steel fiber reinforced concrete subjected to drop weight test, Cement Concrete Research 29 (1999) 989–995.
[5] B. Arisoy, H.C. Wu, Material characteristics of high performance lightweight concrete reinforced with PVA, Construction and Building Materials 22 (4) (2008) 635–645.
[6] K. Friedrich, S. Fakirov, Z. Zhang, Polymer Composites: From Nano-to-macro-scale, Springer Inc., New York, pp. 129-130.
[7] S. Zhandarov, E. Ma¨der, Characterization of fiber/matrix interface strength: applicability of different tests, approaches and parameters, Composites Science and Technology 65 (2005) 149–160.
[8] T. Akçaolu, M. Tokyay, T. Çelik, Effect of coarse aggregate size on interfacial cracking under uniaxial compression, Materials Letters, Vol. 57, No. 4, pp. 828-833.
[9] T. Akçaolu, M. Tokyay, T. Çelik, Effect of coarse aggregate size and matrix quality on ITZ and failure behavior of concrete under uniaxial compression, Cement and Concrete Composites, Vol. 26, No. 6, pp. 633-638.
[10] W.A. Tasong, C.J. Lynsdale, J.C. Cripps, Aggregate-cement paste interface: Part I. Influence of aggregate geochemistry. Cem. Concr. Res. Vol. 29, pp. 1019-1025.
[11] D.P. Bentz, Influence of silica fume on diffusivity in cement-based materials. II. Multi-scale modeling of concrete diffusivity, Cement and Concrete Research 30 (7), 1121-1129.
[12] A.H. Asbridge, G.A. Chadbourn, C.L. Page, Effects of metakaolin and the interfacial transition zone on the diffusion of chloride ions through cement mortars. Cement and Concrete Research 31 (11), 1567-1572.
[13] C. Poon, L. Lam, S.C. Kou, Y. Wong, R. Wong, Rate of pozzolanic reaction of metakaolin in high-performance cement pastes, Cement and Concrete Research 31, 1301-1306.
[14] H. Toutanji, B. Xu, J. Gilbert, T. Lavin, Fracture toughness model for poly(vinyl alcohol) fiber reinforced high-performance cementitious material, Proceedings: 8th International Symposium on Utilization of High-Strength and High-Performance Concrete, Tokyo, Japan, 2008, p. 9, Paper No.133.
[15] T. Lavin, H. Toutanji, B. Xu, T. Ooi, K. Biszick, J. Gilbert, Matrix design for strategically tuned absolutely resilient structures (STARS), Proceedings: SEM XI International Congress & Exposition on Experimental and Applied Mechanics, Orlando, FL, 2008, p. 12, Paper No. 71.
[16] J.E. Mark, Polymer Data Handbook, Oxford University Press, Inc, 1999, pp. 910–912.
[17] D. Feldman, A. Barbalata, Synthetic Polymers: Technology, Properties, Applications, Chapman and Hall, London, 1991, p. 101.
[18] K.K. Chawla, Composite Materials science and Engineering, Springer-Verlag, New York, Page:234-236.
[19] ASTM C618, Standard specification for coal fly ash and raw or calcined natural pozzolan for use in concrete, American Society for Testing and Materials Standards Annual Books, Vol.04.02.
[20] ASTM C494, Standard Specification for Chemical Admixtures for Concrete, American Society for Testing and Materials Standards Annual Books, Vol.04.02.
[21] ASTM E23, Standard Test Methods for Notched Bar Impact Testing of Metallic Materials.
[22] C.H. Hsueh, Crack-wake interfacial debonding criteria for fiber-reinforced ceramic composites, Acta Materialia 44 (6) (1996) 2211–2216 June.
[23] J.P. Favre, G. Désarmot, O. Sudre, A. Vassel, Were McGarry or Shiriajeva right to measure glass–fiber adhesion? Compos Interfaces 4 (1997) 313–326.
[24] T. Kanda, V.C. Li, Interface property and apparent strength of high-strength hydrophilic fiber in cement matrix, J Mater Civil Eng 10 (1998) 5–13.
[25] Z. Sun, E.J. Garboczi, S.P. Shah, Modeling the elastic properties of concrete composites: experiment, differential effective medium theory, and numerical simulation, Cement and Concrete Composites 29 (1) (2007) 22–38.
[26] T. Kanda, V.C. Li, Practical design criteria for saturated pseudo strain hardening behavior in ECC, Journal of advanced concrete technology 4 (1) (2006) 59–72.